

## ESR Identification of Free Radicals Formed from the Oxidation of Catechol Estrogens by $\text{Cu}^{2+}$

Andrew M. Seacat,<sup>\*1</sup> Periannan Kuppusamy,<sup>†</sup> Jay L. Zweier,<sup>†</sup> and James D. Yager<sup>\*2</sup>

<sup>\*</sup>*Division of Toxicological Sciences, Department of Environmental Health Sciences, Johns Hopkins University School of Hygiene and Public Health, 615 N. Wolfe Street, Baltimore, Maryland 21205-2179; and* <sup>†</sup>*The Molecular and Cellular Biophysics Laboratories, Department of Medicine, Division of Cardiology and the Electron Paramagnetic Resonance Center, Johns Hopkins Medical Institutions, 5501 Hopkins Bayview Circle, Baltimore, Maryland 21224*

Received May 9, 1997, and in revised form July 30, 1997

**Catechol estrogens are genotoxic, indirectly through redox cycling mechanisms leading to oxidative DNA damage and directly by formation of quinone–DNA adducts. Previously, we demonstrated that  $\text{Cu}^{2+}$  can oxidize estradiol (E2) catechols, establishing a copper redox cycle leading to the formation of DNA strand breaks. The goal of this study was to use electron spin resonance techniques to identify the free radical intermediates formed. The 2- and 4-OH catechols of E2 and ethinyl estradiol (EE) were oxidized to semiquinone intermediates, stabilized by  $\text{Mg}^{2+}$ , when incubated with  $\text{Cu}^{2+}$ . The 4-OH-EE semiquinone decayed more slowly than the 2-OH-EE semiquinone. Using the spin trap  $\alpha$ -(4-pyridyl-1-oxide)-*N*-tert-butyl nitron, 4-OH-E2 plus  $\text{Cu}^{2+}$  generated hydroxyl radicals at a greater rate than 2-OH-E2 plus  $\text{Cu}^{2+}$ . Formation of hydroxyl and methyl radical adducts was detected, using 5,5-dimethyl-1-pyrroline-*N*-oxide as the spin trap, when 2-OH-E2 was incubated with  $\text{Cu}^{2+}$  and 1% dimethyl sulfoxide. This was inhibited by the  $\text{Cu}^{1+}$  chelator bathocuproinedisulfonic acid and catalase. These data demonstrate that the oxidation of estrogen catechols by  $\text{Cu}^{2+}$  leads to a Cu-dependent mechanism of hydroxyl radical production via a hydrogen peroxide intermediate and suggest a mechanism for estrogen-associated site-specific DNA damage and mutagenesis.** © 1997 Academic Press

**Key Words:** catechol estrogens; redox cycle; copper; DNA; reactive oxygen; free radicals.

An increased risk for developing several common cancers in women, including breast, endometrium, ovary, and liver, has been linked to cumulative exposure to endogenous and synthetic estrogens (1–4). In general, the main mechanism put forth to account for estrogen carcinogenicity has been estrogen receptor-mediated, persistent cell proliferation associated with spontaneous replication errors (2). While estrogen-induced cell proliferation undoubtedly has an important role in the carcinogenic process, mounting evidence supports a complementary pathway involving indirect and direct genotoxicity originating from estrogen metabolites, in particular the 4-OH catechol of estradiol (3). The indirect effects, reflected by increased oxidative DNA damage, arise from redox cycling of the catechol metabolites which generates reactive oxygen species (ROS),<sup>3</sup> while the direct effects are due to the formation of quinone–DNA adducts (3).

Reactive oxygen species have been shown to be involved in all stages of carcinogenesis from the activation of carcinogens during initiation through promotion and progression (5, 6). The hydroxyl radical is highly reactive at many sites on DNA and has been shown to react with guanosine at the C-8 position to form 8-oxo-deoxyguanosine (8-oxo-dG) (7). The 8-oxo-dG adduct is capable of mispairing with adenine or thymine and causing a G to T transversion or a G to A transition, respectively (8). Copper has been found complexed with guanine (G) bases in DNA (9) and poly G sites are particularly sensitive to cleavage by ROS (10). Proposed reactions include hydrogen peroxide interacting

<sup>1</sup> Present address: Toxicological Services, 3M Medical Department, 3M Center, Building 220-2E-02, P.O. Box 33220, St. Paul, MN 55133-3220.

<sup>2</sup> To whom correspondence should be addressed at Division of Toxicological Sciences, Department of Environmental Health Sciences, Johns Hopkins University School of Hygiene and Public Health, Room 7032, 615 N. Wolfe Street, Baltimore, MD 21205-2179. Fax: 410-955-0116. E-mail: jyager@sph.jhu.edu.

<sup>3</sup> Abbreviations used: ROS, reactive oxygen species; ESR, electron spin resonance; EE, ethinyl estradiol; PBS, phosphate-buffered saline; DMPO, 5,5-dimethyl-1-pyrroline-*N*-oxide; POBN,  $\alpha$ -(4-pyridyl-1-oxide)-*N*-tert-butyl nitron; BCS, bathocuproinedisulfonic acid; DMSO, dimethyl sulfoxide; SOD, superoxide dismutase.

with DNA-bound copper ions to yield Cu(I)-peroxy intermediates leading to DNA strand breaks and reduction by semiquinones to yield hydroxyl radicals and the quinones (10). Superoxide may react with itself or with hydroxyl radicals to form singlet oxygen (11), which is highly reactive and is also capable of causing DNA strand breaks and forming 8-oxo-dG (12–14).

Redox cycling of the catechol estrogens to their *o*-quinone forms by a cytochrome P450 oxidase and NADPH-dependent cytochrome P450 reductase system is accompanied by the generation of reactive oxygen species (15–18) that can cause oxidative DNA damage (3, 15). Alternatively, catechol estrogens can be activated to reactive intermediates by metal-catalyzed autooxidation (19). It has been shown that Cu<sup>2+</sup>-mediated oxidation of several catechol containing xenobiotics causes the formation of ROS capable of forming DNA strand breaks (20, 21). For example, reaction of 2-hydroxy-estradiol (2-OH-E2) plus Cu<sup>2+</sup> causes DNA strand breaks through a Cu<sup>2+</sup>/Cu<sup>1+</sup> redox cycle, which generates superoxide and hydrogen peroxide as intermediates (21).

Electron spin resonance (ESR) spectroscopy has been used to identify free radical metabolites of xenobiotics *in vivo* and to study their chemistry *in vitro* (22). The purpose of using ESR in this study was to definitively identify the free radicals produced by the catechol estrogen/copper redox system. The oxidation of catechol estrogens to their quinone form by copper has previously been suggested to occur via a semiquinone intermediate (21). The semiquinone intermediate, upon reacting with oxygen, forms superoxide and the quinone product, thus initiating a Cu<sup>2+</sup>/Cu<sup>1+</sup> redox cycle leading to DNA damage. The data presented here provide direct evidence for the formation of a semiquinone intermediate and ROS by this nonenzymatic mechanism.

## MATERIALS AND METHODS

**ESR spectra.** ESR spectra were recorded on a Burkert ER-300 ESR spectrometer (Billerica, MA) operating at X-band with a TM flat cell at room temperature. The spectrometer settings were modulation frequency, 100 kHz; modulation amplitude, 0.5 G; scan time, 30 s; microwave power 20 mW; and microwave frequency, approximately 9.778 GHz. Spectral simulations were matched with experimental data to extract the spectral parameters. The catechol estrogens were always added last, immediately before loading the solution into the flat cell, which was then placed into the ESR cavity. Thirty to 90 s from the start of the reaction was required for loading and tuning the instrument.

**Catechol estrogen-copper reaction system.** The reaction conditions for catechol estrogen-derived ROS and their measurement by ESR were similar to previously published methods (23). The catechol estrogens used in this study were 2-OH- and 4-OH-E2 and 2-OH- and 4-OH-ethinyl estradiol (EE). The latter is a component of oral contraceptives and is a strong liver tumor promoter and weak complete hepatocarcinogen (3). The estradiol catechols were purchased from either Sigma Chemical Co. (St. Louis, MO) or Steraloids (Wil-

ton, NH), while the ethinyl estradiol catechols were synthesized as described by Gelbke *et al.* (24). The catechol estrogens (200 μM) were incubated with 10 μM CuSO<sub>4</sub> and 0.5 M MgCl<sub>2</sub> in 600 μL phosphate-buffered saline (PBS).

**Semiquinone and ROS detection.** The semiquinones were detected directly as their Mg<sup>2+</sup>-stabilized forms as described previously (25).

The spin traps 5,5-dimethyl-1-pyrroline-*N*-oxide (DMPO) and  $\alpha$ -(4-pyridyl)-1-oxide)-*N*-*tert*-butyl nitron (POBN) were used to detect ROS. DMPO (1 M) in chelexed (stock) water was added to the incubation mixtures in 1× PBS to a final concentration of 50 mM. POBN (1 M) was made up in chelexed water in the dark immediately before use at a final concentration of 30 mM. All spectra and data shown are representative of experiments repeated at least two times.

## RESULTS

**Detection of the semiquinones.** Incubation of 2- and 4-OH catechol estrogens of both E2 and EE with 10 μM Cu<sup>2+</sup> results in formation of their semiquinones. Representative spectra are shown in the figures. Figures 1A and 1B show the ESR signals from the copper-

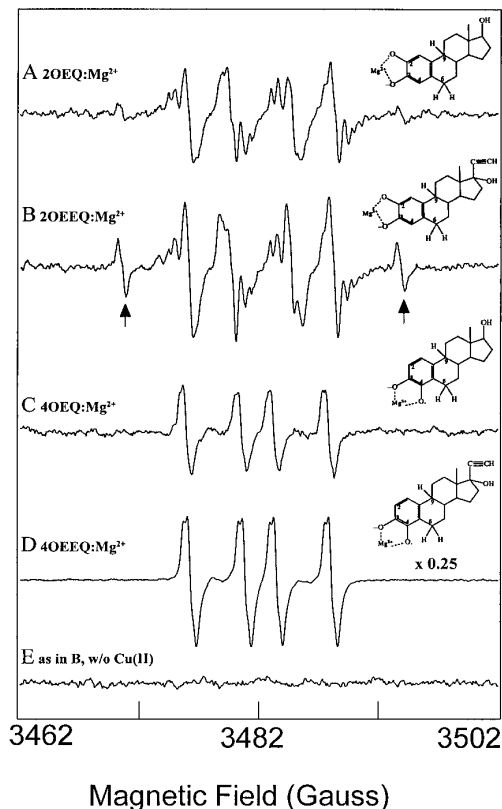


**FIG. 1.** ESR spectra of Mg<sup>2+</sup>-stabilized 2- and 4-*o*-semiquinone radicals from catechol estrogens in the presence of Cu<sup>2+</sup>. Catechol estrogens (200 μM) were incubated with 10 μM CuSO<sub>4</sub> and 0.5 M MgCl<sub>2</sub> in 600 μL PBS for 20 min: (A) 2-OH-E2, (B) 2-OH-EE, (C) 4-OH-E2, (D) 4-OH-EE. Arrows point to peaks of widest splitting caused by the hydrogen at C-9 found only in the 2-hydroxy-derived semiquinones. The dependence on copper is shown in E where Cu<sup>2+</sup> was not added but 10 μM BCS was, to chelate any contaminating copper.

**TABLE I**  
ESR Parameters of  $\text{Cu}^{2+}$ -Catalyzed  $\phi$ -Semiquinones  
from Catechol Estrogens

Radical <sup>a</sup>	Hyperfine splittings (G)				g
	$a_{\text{H}(C-6)}$	$a_{\text{H}'(C-6)}$	$a_{\text{H}(C-9)}$	$a_{\text{H}(\text{aromatic})}$	
2-OEQ: $\text{Mg}^{2+}$	8.46	5.71	9.30	0.3	2.0042
4-OEQ: $\text{Mg}^{2+}$	—	—	7.27 <sup>b</sup>	4.65	2.0042

<sup>a</sup> For structures see Fig. 1.

<sup>b</sup> The largest hyperfine splitting for 4-OEQ: $\text{Mg}^{2+}$  is tentatively assigned to the proton at C-9, as per the work of Kalyanaraman *et al.* (25).

catalyzed,  $\text{Mg}^{2+}$ -stabilized formation of the 2-OH-E2 semiquinone (2-OEQ: $\text{Mg}^{2+}$ ) and 2-OH-EE semiquinone (2-OEEQ: $\text{Mg}^{2+}$ ), respectively. One can see the similarity between the two spectra, with the salient characteristic being the outermost splitting (indicated by arrows). The 4-hydroxyestrogen semiquinones 4-OEQ: $\text{Mg}^{2+}$  and 4-OEEQ: $\text{Mg}^{2+}$  (Figs. 1C and 1D) are formed from oxidation of the 4-OH catechols by  $\text{Cu}^{2+}$ . The 4-OH-estrogen semiquinones lose the C-6 hyperfine splitting contribution, leaving a four-line spectra. The amplitudes of the ESR spectra of the EE-derived semiquinones were greater than those of the E2 equivalents. In particular, this was true for the 4-OEEQ: $\text{Mg}^{2+}$  which is shown at  $\frac{1}{4}$  scale (Fig. 1D). Figure 1E indicates the absence of semiquinone formation when no copper was added and 10  $\mu\text{M}$  bathocuproinedisulfonic acid (BCS) was present to chelate any contaminating  $\text{Cu}^{1+}$ .

The ESR spectra shown in Fig. 1 and their hyperfine coupling constants (Table I) are similar to those obtained by  $\text{Mg}^{2+}$  stabilization of catechol estrogen quinones formed by enzymatic methods or autooxidation of the catechol by a strong base (25). For the  $\text{Mg}^{2+}$ -stabilized semiquinone of 2-OH-E2, the  $\beta$ -cyclic protons at C-6 and C-9 cause three hyperfine couplings with a small splitting contribution from the aromatic hydrogen. For the 4-OH semiquinone, the hydrogen at C-9 is the major contributor to the hyperfine coupling, followed by a contribution from the aromatic hydrogen at the C-2 position. The C-6 hydrogens cause only a minor splitting, seen at the tops of the four major peaks (25). The 7.27 G splitting assignment to C-9 was previously determined based on the evidence that OH substitution at C-6 did not affect the observed spectra (25). The hyperfine splitting values for the EE 2- and 4-semiquinones were identical to the values for the E2 2- and 4-semiquinones (25).

*Detection of free radicals using DMPO as a spin trap.* ESR spectra of hydroxyl and methyl radicals produced by incubation of 100  $\mu\text{M}$  2-OH-E2 with 10  $\mu\text{M}$  copper and dimethyl sulfoxide (DMSO) and spin-trapped with

DMPO are shown in Fig. 2. The complete system (A) yields a 1:1:1:1:1 sextet ( $a_{\text{N}} = 15.3$  G,  $a_{\text{H}} = 22.0$  G), characteristic of the DMPO–methyl (DMPO- $\text{CH}_3$ ) radical spin adduct, with an interspersed 1:2:2:1 quartet ( $a_{\text{N}} = a_{\text{H}} = 14.85$  G), typical of the DMPO–hydroxyl (DMPO-OH) radical adduct. Methyl radicals are produced by the reaction of hydroxyl radicals with DMSO and are in turn trapped by DMPO (26). A minor contribution from an unknown radical adduct (DMPO-X) is also observed (Fig. 2A).

Figure 2B shows the spontaneous formation of the DMPO-OH radical adduct when 2-OH-E2 is removed from the complete system. Identical spectra to those shown in Fig. 2B were seen when DMSO was removed from the complete system and when DMPO and 10  $\mu\text{M}$   $\text{Cu}^{2+}$  were incubated together, without DMSO (data not shown). A nonradical nucleophilic, metal-catalyzed addition of water to DMPO may account for these re-

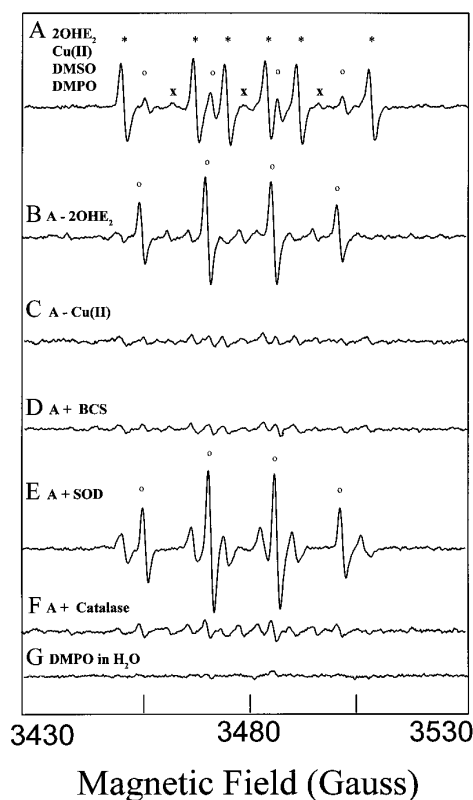


**FIG. 2.** ESR spectra of methyl (\*), hydroxyl (O), and unknown (x) free radicals produced by incubation of catechol estrogens with copper and spin-trapped with 5,5-dimethyl-1-pyrroline-*N*-oxide (DMPO). (A) Complete system with 100  $\mu\text{M}$  2-OH-E2, 10  $\mu\text{M}$   $\text{CuSO}_4$ , 1% DMSO, and 50 mM DMPO; (B) complete system minus 2-OH-E2; (C) complete system minus  $\text{CuSO}_4$ ; (D) complete system plus 40  $\mu\text{M}$  BCS; (E) complete system plus 1000 U/ml superoxide dismutase; (F) complete system plus 500 U/ml catalase; (G) 50 mM DMPO in chelated water. After adding the catechol estrogen, the ESR spectra were repetitively acquired for 30 min. These spectra represent averaged ESR signals from 10 scans of 30 s each.

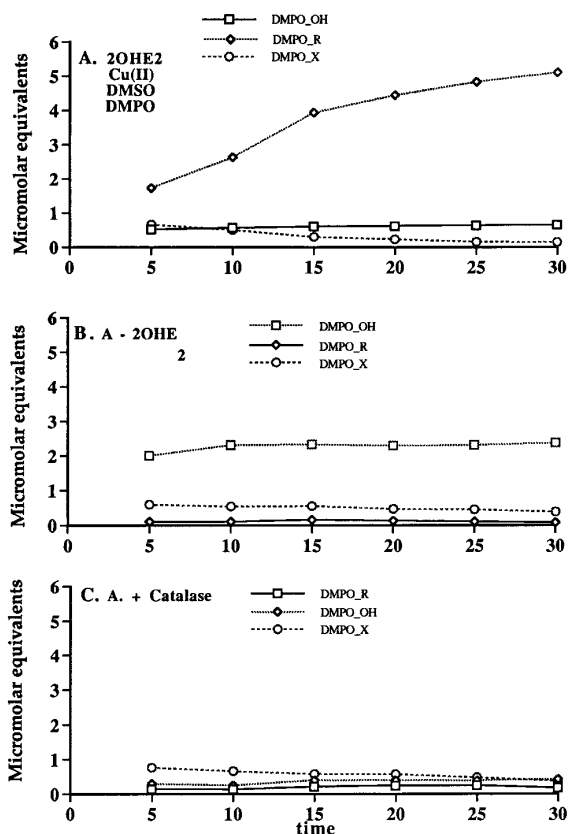


**FIG. 3.** Time course of development of the DMPO adducts formed by 2-OH-E2 plus  $\text{Cu}^{2+}$  from the spectra seen in Fig. 2A. (A) Formation of a DMPO-hydroxyl adduct (DMPO\_OH), a DMPO-methyl (or alkyl) adduct (DMPO\_R), and an unidentified DMPO adduct (DMPO\_X); (B) formation of hydroxyl-, methyl-, and X-DMPO adducts from Fig. 2B (complete system minus 2-OH-E2); (C) formation of the DMPO adducts from Fig. 2F (complete system plus 500 U/ml catalase).

sults (27, 28). The removal of copper (Fig. 2C) or its chelation by BCS (Fig. 2D) blocked the formation of both DMPO- $\text{CH}_3$  and DMPO-OH. These data indicate the necessity of a  $\text{Cu}^{1+}/\text{Cu}^{2+}$  redox cycle for the formation of these spin adducts. Addition of 500 U/ml Cu,Zn-superoxide dismutase (CuZn-SOD) enhanced the formation of DMPO-OH, but inhibited the production of DMPO- $\text{CH}_3$  (Fig. 2E). The formation of the DMPO- $\text{CH}_3$  was nearly completely blocked by 500 U/ml catalase (Fig. 2F), indicating the involvement of  $\text{H}_2\text{O}_2$  in the generation of this spin adduct. However, the formation of the DMPO-OH was only slightly inhibited by catalase (Fig. 2F), further supporting the notion that the DMPO-OH was formed by the nonradical nucleophilic addition of  $\text{H}_2\text{O}$ . DMPO, in chelexed water, had no ESR signal (Fig. 2G).

The rates of formation for each of the three DMPO adducts formed in the reactions shown in Figs. 2A, 2B, and 2F are shown in Figs. 3A, 3B, and 3C, respectively. True zero times were not recorded due to the require-

ment for premixing, loading, and tuning the instrument before the first measurement could begin. The first point represents the cumulative data for the first 5 min of recording. Note that in the presence of DMSO (Fig. 3A), the methyl adduct (DMPO- $\text{CH}_3$ ) exhibited a time-dependent increase through the 30-min period of incubation (Fig. 3A), revealing the continued production of hydroxyl radicals from the  $\text{Cu}^{2+}$ -catalyzed oxidation of 2-OH-E2. This is consistent with our previous observation that the production of  $\text{H}_2\text{O}_2$  from 2-OH-E2/ $\text{Cu}^{2+}$  was time dependent (21). Other experiments, where this reaction was followed for more than 1.5 h, showed a continued increase up to after 45 min, followed by a gradual decline (data not shown), which most likely represented degradation of the spin trap and depletion of substrate. The "spontaneous" formation of the DMPO-OH signal in the system, without catechol estrogens, remained at a steady level over the time measured (Fig. 3B). The time-dependent increase of DMPO- $\text{CH}_3$  adducts in the complete system was also totally abolished by catalase (Fig. 3C), again suggesting a peroxide intermediate. Catalase had little effect on the DMPO-OH and the constitutive background of the unidentified radical adduct DMPO-X (Fig. 3C).

The spectral parameters for the three DMPO adducts generated by the catechol estrogen/ $\text{Cu}^{2+}$  system shown in Fig. 2A were derived by computer simulation. The experimental spectrum is shown again in Fig. 4A. Simulated spectra for the individual components of the experimental spectrum and its composites are shown in Figs. 4B–4E. The spectral parameters of each component are DMPO- $\text{CH}_3$ :  $a_N = 16.31$  G,  $a_H = 23.53$  G; DMPO-OH:  $a_N = a_H = 14.85$  G; and DMPO-X:  $a_N = 16.85$  G. These values for the hydroxyl- and methyl-DMPO adducts are in close agreement with published values, given the variable effect that the local ionic environment can have on splitting constants (29).

*Detection of free radicals using POBN as a spin trap.* Both the pyrroline (DMPO) and the aryl (POBN) nitrones can undergo hydrolysis to give rise to nitroxides; however, DMPO is more susceptible to decomposition by light and oxygen (26). Experimentally, POBN proved to be superior for these applications since it is not subject to metal-catalyzed addition of water, as is DMPO (27). The addition of 2-OH-E2 to a solution containing  $\text{CuSO}_4$ , DMSO, and POBN results in an ESR spectrum consisting of a triplet of doublets (Fig. 5A) arising from the POBN- $\text{CH}_3$  adduct. Hydroxyl radicals add to DMSO and the resulting alkoxy radicals decompose to methyl radicals, which are efficiently scavenged by POBN (30). Removal of DMSO from the incubation eliminates the signal, showing that the spontaneous signals seen with copper and DMPO are not present with copper and POBN (Fig. 5B). Addition of 1 mM GSH abolished the formation of the POBN-

$\text{CH}_3$  adduct (Fig. 5C), a result observed by others with hydroquinone (31). As expected, 4-OH-E2 also generated hydroxyl radicals, as indicated by the formation of POBN- $\text{CH}_3$  adducts in the presence of DMSO (Figs. 5D and 5E).

**Rate of OH radical formation and semiquinone stability.** Next, we compared the rates of hydroxyl radical formation and the decay of  $\text{Mg}^{2+}$ -stabilized semiquinones formed from the 2- and 4-hydroxyestrogens incubated with copper. The results, shown in Fig. 6, were observed in two separate experiments. 4-OH-E2 produced hydroxyl radicals at a faster overall rate than 2-OH-E2 ( $0.26 \mu\text{mol}/\text{min}$  vs  $0.14 \mu\text{mol}/\text{min}$ , respectively), and up to 25 min, to a greater extent (Fig. 6A). In addition, the semiquinone of 4-OH-EE was seen to decay at a slower rate than the semiquinone of 2-OH-EE ( $-1.4 \mu\text{mol}/\text{min}$  vs  $-3.4 \mu\text{mol}/\text{min}$ , respectively) (Fig.

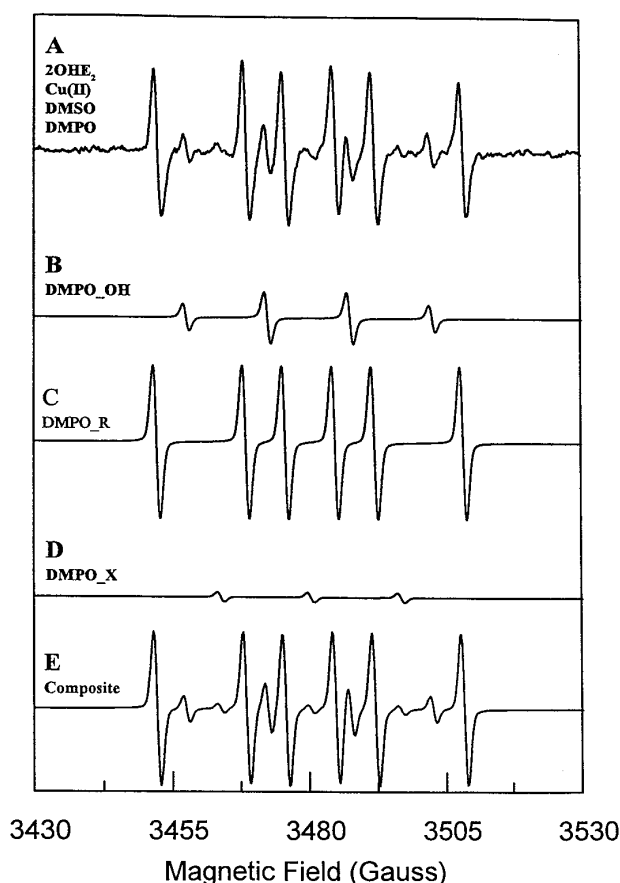


**FIG. 4.** Simulated ESR spectra for the experimental spectra of the DMPO adducts of 2-OH-E2 plus copper-generated radicals. (A) The experimental spectra generated from  $100 \mu\text{M}$  2-OH-E2,  $10 \mu\text{M}$   $\text{CuSO}_4$ , 1% DMSO, and 50 mM DMPO (as in Fig. 2A); (B) simulated spectra of the hydroxyl-DMPO adduct (DMPO-OH); (C) simulated spectra of the alkyl-DMPO adduct (DMPO-R); (D) simulated spectra of the unknown DMPO adduct (DMPO-X); (E) composite-simulated ESR spectra of B-D above.

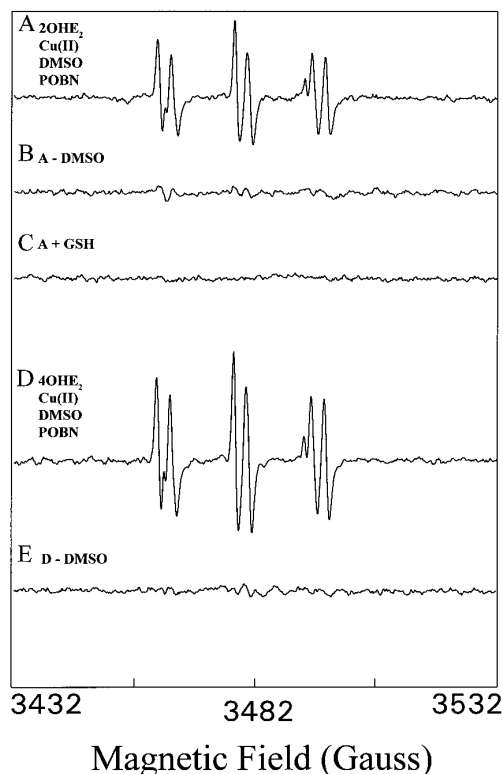


**FIG. 5.** ESR spectra of the POBN- $\text{CH}_3$  adduct generated from the reaction of 2-OH-E2 with  $\text{Cu}^{2+}$  in the presence or absence of DMSO and the effect of reduced glutathione. (A)  $100 \mu\text{M}$  2-OH-E2,  $10 \mu\text{M}$   $\text{CuSO}_4$ , 1% DMSO, 30 mM POBN, and 0.25% DMF; (B) as in A minus DMSO; (C) as in A plus 1 mM GSH; (D)  $100 \mu\text{M}$  4-OH-E2,  $10 \mu\text{M}$   $\text{CuSO}_4$ , 1% DMSO, 30 mM POBN, and 0.25% DMF; (E) as in D minus DMSO.

6B). This combination of an apparently more stable semiquinone and a greater generation of hydroxyl radicals suggests that, based on these properties alone, the 4-hydroxy estrogens may, in the presence of copper, be more potent mediators of oxidative damage than the 2-hydroxyestrogens.

## DISCUSSION

Previously, we demonstrated an alternative, nonenzymatic mechanism for estrogen oxidation (21). In this system, the E2 and EE 2,3- and 3,4-catechols are oxidized by  $\text{Cu}^{2+}$  through a process which generates a  $\text{Cu}^{2+}/\text{Cu}^{1+}$  redox cycle and leads to the generation of ROS that can cause DNA strand breaks. In the current study, we used ESR spectroscopy to identify the radical species formed in this process and found that both the 2-OH- and the 4-OH-catechols of E2 and EE form their respective semiquinone free radical intermediates and ROS when incubated with copper. The magnesium-stabilized semiquinone intermediate of 4-OH-EE was observed to decay at a slower rate than the 2-OH-EE

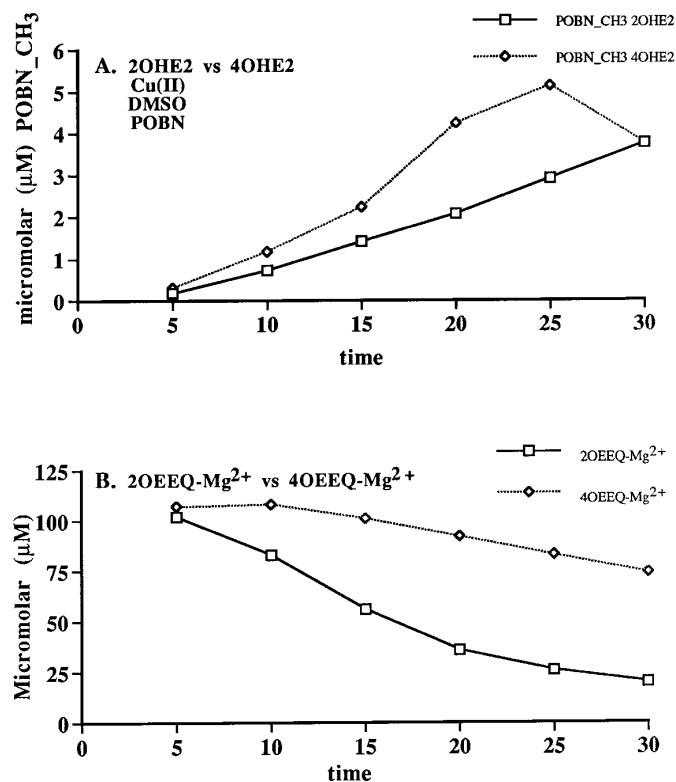


**FIG. 6.** Time course of hydroxyl radical formation and semiquinone stability. (A) POBN-CH<sub>3</sub>-formation from 2-OH-E2 and 4-OH-E2. These kinetic data were derived from the spectra of Figs. 5A and 5D, respectively. (B) Time course of decay of the semiquinones of 2-OH-EE (2-OEEQ-Mg<sup>2+</sup>) and 4-OH-EE (4-OEEQ-Mg<sup>2+</sup>). These kinetic data were derived from EPR spectra shown in Figs. 1B and 1E, respectively.

equivalent. Using the POBN spin trap, we found that hydroxyl radicals were generated at a faster rate from 4-OH-E2 than 2-OH-E2. These findings suggest that the 4-OH-catechol may be of particular significance in estrogen carcinogenesis. In this regard, Han and Liehr noted that 4-OH, but not 2-OH-E2-catechols cause renal tumor formation in Syrian hamsters (32). Furthermore, in a microsome-mediated redox-cycle, 4-OH-E2 also caused oxidative damage to DNA (33). However, in our *in vitro* system, both the 2-OH- and 4-OH-catechols were equally effective in causing oxidative DNA damage (Seacat *et al.*, unpublished observations), suggesting that other factors may also be involved in the increased carcinogenicity of the 4-OH-catechol.

Using the DMPO spin trap in conjunction with DMSO, we observed formation of both DMPO-CH<sub>3</sub> and DMPO-OH adducts from the 2-OH-E2/Cu<sup>2+</sup> system (Fig. 2A). Because Cu<sup>2+</sup> is able to catalyze the nonradical nucleophilic addition of H<sub>2</sub>O to form DMPO-OH adduct (26, 28), the DMPO-OH observed in Fig. 2A is likely to result from such a nucleophilic addition. This is further supported by the ineffectiveness of catalase

on DMPO-OH formation (Fig. 2F). It has been shown that the metal-catalyzed nucleophilic addition of H<sub>2</sub>O to DMPO is not catalase inhibitable (28). The formation of DMPO-CH<sub>3</sub> (Fig. 2A) indicates the production of hydroxyl radicals from the 2-OH-E2/Cu<sup>2+</sup>. Because both H<sub>2</sub>O<sub>2</sub> and Cu<sup>1+</sup> can be formed during the oxidation of 2-OH-E2 by Cu<sup>2+</sup> (21), a Fenton-type reaction between the Cu<sup>1+</sup> and H<sub>2</sub>O<sub>2</sub> appears to be involved in the production of hydroxyl radicals which were detected in the form of DMPO-CH<sub>3</sub> adducts in Fig. 2A. The occurrence of such Fenton-type chemistry was further supported by the complete inhibition of the DMPO-CH<sub>3</sub> formation by either BCS or catalase (Figs. 2D and 2F). The enhancement of the DMPO-OH formation by removal of 2-OH-E2 (Fig. 2B) would suggest that in the complete system, the reaction between Cu<sup>2+</sup> and 2-OH-E2 may dominate and thereby limit the Cu<sup>2+</sup>-catalyzed nucleophilic addition of H<sub>2</sub>O. Addition of SOD enhanced DMPO-OH and decreased DMPO-CH<sub>3</sub> adduct formation (Fig. 2E). This result can be explained because in addition to catalyzing the dismutation of superoxide to H<sub>2</sub>O<sub>2</sub>, Cu,Zn-SOD has a peroxidase function which can result in enzyme-mediated <sup>•</sup>OH formation with the generation of either metal coordinated or free <sup>•</sup>OH (34, 35). DMPO can enter the positively charged active channel of SOD and come into close proximity with the active site where metal coordinated <sup>•</sup>OH, caged <sup>•</sup>OH, or free <sup>•</sup>OH are formed (35). Thus, the peroxidative function of SOD can limit the reaction of free Cu<sup>1+</sup> and H<sub>2</sub>O<sub>2</sub>. Since DMPO can enter the active channel of SOD in a position to intercept <sup>•</sup>OH radicals as they are formed, a large DMPO-OH signal is observed with little DMPO-CH<sub>3</sub>. These factors may explain the decrease of DMPO-CH<sub>3</sub> which was observed in the presence of SOD (Fig. 2E).

The formation of hydroxyl radicals from the Cu<sup>2+</sup>-mediated oxidation of estrogen catechols was also detected by POBN spin trapping, in conjunction with DMSO (Fig. 5). We found that glutathione (1 mM) abolished the formation of the POBN-CH<sub>3</sub> adduct. This would not be caused by a reaction between GSH and the quinones, since the ROS formed in our system are due to the redox cycling of copper and not the estrogen catechols/quinones. Rather, it is likely that the inhibitory effect of GSH was due to its being a potent chelator of Cu<sup>1+</sup>, thus interfering with the reduction of superoxide to H<sub>2</sub>O<sub>2</sub> and of H<sub>2</sub>O<sub>2</sub> to hydroxyl radicals by Cu<sup>1+</sup> (36) and other reactive oxygen species. Indeed, Hanna and Mason observed that the formation of hydroxyl radical adduct of DMPO from copper/H<sub>2</sub>O<sub>2</sub> but not from iron/H<sub>2</sub>O<sub>2</sub> was abolished by GSH (37).

Generation of hydrogen peroxide by antitumor quinones redox cycling with copper has been shown to increase oxidative DNA base damage *in vitro* and *in vivo* (38). The oxidation of catechol estrogens to semiquinones or of hydroquinone to benzoquinone by a

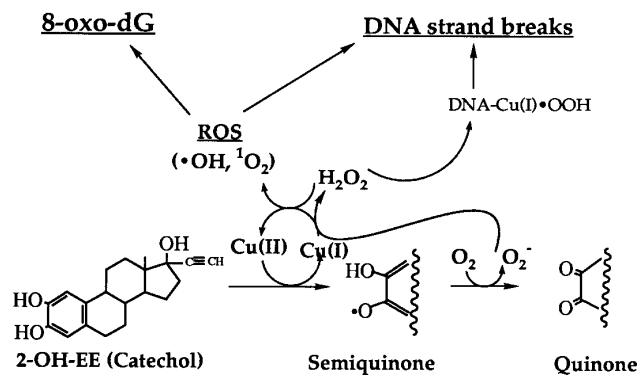


**FIG. 7.** Scheme for the  $\text{Cu}^{2+}/\text{Cu}^{1+}$ -mediated oxidation of catechol estrogens.

$\text{Cu}^{2+}/\text{Cu}^{1+}$  redox cycle has been shown to cause DNA strand breaks (21, 39). In the hydroquinone to benzoquinone system, hydroxyl radicals or equivalent species were formed, as shown by ESR (31). The generation of reactive oxygen species by the redox cycling of quinones and the requirement of transition metals in that reaction have been reviewed recently (40–42). What many authors refer to as autooxidation between biomolecules and oxygen to yield superoxide, hydrogen peroxide, and hydroxyl radicals is in all probability catalyzed by metals bound to the biomolecules (42).

The interactions of these radicals with each other and with DNA are complex. Superoxide can interact with the catechol estrogen to yield semiquinone and hydrogen peroxide (43). Hydrogen peroxide can also oxidize the catechol estrogens to their semiquinones and can give rise to singlet oxygen (43). Hydrogen peroxide and  $\text{Cu}^{1+}$  have been proposed to form a strong oxidizing  $\text{Cu}^{3+}$  species capable of attacking DNA. Kinetic studies of the reaction of  $\text{H}_2\text{O}_2$  and  $\text{Cu}^{1+}$ , which by the Fenton-type reaction should yield hydroxyl radicals, support the formation of  $\text{Cu}(\text{III})$  instead (44, 45). Since both  $\text{Cu}^{3+}$  and  $\cdot\text{OH}$  can oxidize DMSO (46), a POBN/DMSO spin-trapping technique cannot readily distinguish between the two radicals (30).

Thus, we see in Fig. 7 that the formation of superoxide by catechol estrogens and copper can theoretically lead to the formation of singlet oxygen and hydroxyl radicals, all of which can oxidatively damage DNA. Furthermore, copper has been shown to bind to DNA preferentially at poly G and GC sequences and it has been shown that copper can mediate the formation of site-specific (sequence context-dependent) oxidative DNA damage (10). It is likely that estrogen catechols can enter the nucleus and reach a  $\text{Cu}^{2+}$ -enriched region of DNA, either alone or, since they are estrogenic (3), bound to the estrogen receptor. In the later instance, it is possible that site-specific oxidative DNA damage could be focused in the promoter regions of

estrogen-responsive genes; this possibility requires investigation.

The oxidative metabolism of estradiol can follow two major pathways (3). A  $17\text{-}\alpha$ -dehydrogenase and  $16\text{-}\alpha$ -hydroxylase act sequentially to form  $16\text{-}\alpha$ -OH estrone which has been reported to bind covalently to proteins, including the estrogen receptor, and to be genotoxic (see 3, for references). Alternatively, several cytochrome P450 isoforms including CYP 1A1 and 3A catalyze hydroxylation at the 2 position, while CYP 1B1 catalyzes hydroxylation at the 4 position of estradiol to form the 2,3- and 3,4-catechols, respectively (3). These catechols are capable of participating in cytochrome P450 oxidase/reductase-mediated redox cycling reactions and, as we have shown, support a  $\text{Cu}^{2+}/\text{Cu}^{1+}$  redox cycle to generate reactive oxygen species and also quinone metabolites which can cause oxidative DNA damage and formation of DNA adducts, respectively. Thus, estrogen metabolites are indirectly and directly genotoxic. Increased oxidative DNA damage has been detected in human breast tumor tissue (47) and in liver DNA of rats treated with ethinyl estradiol (48). Furthermore, recent evidence indicates that the 4-hydroxy-catechol estrogens can react with cellular thiols to form highly reactive quinone methides to a greater extent than do the 2-hydroxy catechols (49). These findings together with those of Liehr and co-workers mentioned above provide support for a role of redox cycling supported by estrogen catechols, particularly the 4-OH E<sub>2</sub>, in the carcinogenic process.

In summary, using ESR spectroscopy we have demonstrated the formation of estrogen semiquinones and hydroxyl radicals in an *in vitro* system where estrogen catechols are oxidized by  $\text{Cu}^{2+}$  and where the subsequent formation of the estrogen quinones is associated with the formation of  $\text{H}_2\text{O}_2$ . The subsequent oxidation of  $\text{Cu}^{1+}$  to  $\text{Cu}^{2+}$  generates more reactive ROS and establishes a copper redox cycle limited only by the concentration of catechol estrogen (Fig. 7). Whether such a process contributes to the indirect genotoxicity of catechol estrogens needs investigation.

## ACKNOWLEDGMENTS

This research was supported by PHS, NIH Grants CA 36701, ES 03819, ES 07141, and HL 38324. In addition, the authors thank Dr. Michael Trush and especially Dr. Yunbo Li for their critical review of the manuscript and helpful suggestions.

## REFERENCES

- Henderson, B. E., Ross, R., and Bernstein, L. (1988) *Cancer Res.* **48**, 246–253.
- Feigelson, H. S., and Henderson, B. E. (1996) *Carcinogenesis* **17**, 2279–2284.
- Yager, J. D., and Liehr, J. G. (1996) *Annu. Rev. Pharmacol. Toxicol.* **36**, 203–232.
- Li, J. J., Kirkman, H., and Li, S. A. (1992) *in* Hormonal Carcino-

- genesis (Li, J. J., Nandi, S., and Li, S. A., Eds.), pp. 217–224, Springer-Verlag, New York.
5. Trush, M. A., and Kensler, T. W. (1991) *Free Rad. Biol Med.* **10**, 201–209.
  6. Egner, P. A., Taffe, B. G., and Kensler, T. W. (1987) in *Biology of Copper Complexes* (Sorenson, J. R. J., Ed.), pp. 413–424, Humana Press, Clifton.
  7. Floyd, R. A. (1990) *Carcinogenesis* **11**, 1447–1450.
  8. Culp, S. J., Cho, B. P., Kadulabar, F. F., and Evans, F. E. (1989) *Chem. Res. Toxicol.* **2**, 416–422.
  9. Kagawa, T. F., Geierstanger, B. H., Wang, A. H.-J., and Ho, P. S. (1991) *J. Biol. Chem.* **266**, 20175–20184.
  10. Sagripanti, J.-L., and Kraemer, K. H. (1989) *J. Biol. Chem.* **264**, 1729–1734.
  11. Kappus, H. (1987) *Arch. Toxicol.* **60**, 144–149.
  12. Devasagayam, T. P. A., Steenken, S., Obendorf, M. S. W., Schulz, W. A., and Sies, H. (1991) *Biochemistry* **30**, 6283–6289.
  13. Lutgerink, J. T., van den Akker, E., Smeets, I., Pachen, D., van Dijk, P., Aubry, J. M., Joenje, H., Lafleur, V. M., and Retel, J. (1992) *Mutat. Res.* **275**, 377–386.
  14. Sies, H., and Menke, C. F. M. (1992) *Mutat. Res.* **275**, 367–375.
  15. Liehr, J. G., and Roy, D. (1990) *Free Radical Biol. Med.* **8**, 415–423.
  16. Liehr, J. G., Ulubelen, A. A., and Strobel, H. W. (1986) *J. Biol. Chem.* **261**, 16865–16870.
  17. Liehr, J. G., Purdy, R. H., Baran, J. S., Nutting, E. E., Oberley, E., Randerath, E., and Randerath, K. (1987) *Cancer Res.* **47**, 2583–2588.
  18. Roy, D., and Liehr, J. G. (1988) *J. Biol. Chem.* **263**, 3646–3651.
  19. Kalyanaraman, B., Hintz, P., and Sealy, R. C. (1986) *FASEB J.* **45**, 2477–2484.
  20. Li, Y., and Trush, M. A. (1993) *Carcinogenesis* **14**, 1303–1311.
  21. Li, Y., Trush, M. A., and Yager, J. D. (1994) *Carcinogenesis* **15**, 1421–1427.
  22. Mason, R. P. (1982) in *Free Radicals in Biology* (Pryor, W. A., Ed.), pp. 161–190, Academic Press, New York.
  23. Stoyanovsky, D. A., Goldman, R., Claycamp, H. G., and Kagan, V. E. (1995) *Arch. Biochem. Biophys.* **317**, 315–323.
  24. Gelbke, H. P., Ball, P., Haupt, O., and Knuppen, P. (1973) *Steroids* **22**, 151–152.
  25. Kalyanaraman, B., Sealy, R. C., and Sivarajah, K. (1984) *J. Biol. Chem.* **259**, 14018–14022.
  26. Rosen, G. M., and Rauckman, E. J. (1984) *Methods Enzymol.* **105**, 198–209.
  27. Burkitt, M. J., Tsang, S. Y., Tam, S. C., and Bremner, I. (1995) *Arch. Biochem. Biophys.* **323**, 63–70.
  28. Hanna, P. M., Chamulitrat, W., and Mason, R. P. (1992) *Arch. Biochem. Biophys.* **296**, 640–644.
  29. Ellington, S. P., Strauss, K. E., and Rosen, G. M. (1988) in *Cellular Antioxidant Defense Mechanisms* (Chow, C. K., Ed.), pp. 41–57, CRC Press, Boca Raton.
  30. Gunther, M. R., Hanna, P. M., Mason, R. P., and Cohen, M. S. (1995) *Arch. Biochem. Biophys.* **316**, 515–522.
  31. Li, Y., Kuppasamy, P., Zweier, J. L., and Trush, M. A. (1995) *Chem.-Biol. Interact.* **94**, 101–120.
  32. Han, X., and Liehr, J. G. (1994) *Carcinogenesis* **15**, 997–1000.
  33. Han, X., and Liehr, J. G. (1995) *Carcinogenesis* **16**, 2571–2574.
  34. Hodgson, E. K., and Fridovich, I. (1975) *Biochemistry* **14**, 5299–5303.
  35. Yim, M. B., Chock, P. B., and Stadtman, E. R. (1993) *J. Biol. Chem.* **268**, 4099–4105.
  36. Milne, L., Nicotera, P., Orrenius, S., and Burkitt, M. J. (1993) *Arch. Biochem. Biophys.* **304**, 102–109.
  37. Hanna, P. M., and Mason, R. P. (1992) *Arch. Biochem. Biophys.* **295**, 205–213.
  38. Muniz, P., Valls, V., Perez-Broseta, C., Iradi, A., Climent, J. V., Oliva, M. R., and Saez, G. T. (1995) *Free Radical Biol. Med.* **18**, 747–755.
  39. Li, Y., and Trush, M. A. (1993) *Arch. Biochem. Biophys.* **300**, 346–355.
  40. Stohs, S. J., and Bagchi, D. (1995) *Free Radical Biol. Med.* **18**, 321–326.
  41. Powis, G. (1989) *Free Radical Biol. Med.* **6**, 63–101.
  42. Miller, D. M., Buettner, G. R., and Aust, S. D. (1990) *Free Radical Biol. Med.* **8**, 95–108.
  43. Kalyanaraman, B., Felix, C. C., and Sealy, R. C. (1985) *Environ. Health Perspect.* **64**, 185–198.
  44. Johnson, G. R. A., Nazhat, N. B., and Sasdalla-Nazhat, R. A. (1985) *J. Chem Soc. Chem. Commun.* **7**, 407–408.
  45. Sutton, H. C., and Winterbourn, C. C. (1989) *Free Radical Biol. Med.* **6**, 53–60.
  46. Yamamoto, K., and Kawanishi, S. (1989) *J. Biol. Chem.* **264**, 15435–15440.
  47. Malins, D. C., Polissar, N. L., and Gunselman, S. J. (1996) *Proc. Natl. Acad. Sci. USA* **93**, 2557–2563.
  48. Ogawa, T., Higashi, S., Kawarada, Y., and Mizumoto (1995) *Carcinogenesis* **16**, 831–836.
  49. Bolton, J. L., and Shen, L. (1996) *Carcinogenesis* **17**, 925–929.